Nitrate sources and transformation processes in groundwater of a coastal area experiencing various anthropogenic stressors

Lamine Boumaiza[1], Safouan Ben Ammar[2], Romain Chesnaux[3], Randy L. Stotler[1], Bernhard Mayer[4], Frédéric Huneau[5], Karen H. Johannesson[6], Jana Levison[7], Kay Knöller[8], Christine Stumpp[9]

[1] University of Waterloo, Department of Earth and Environmental Sciences, Waterloo, Ontario, N2T 0A4, Canada

[2] Université de Carthage, Institut Supérieur des Technologies de l'Environnement de l'Urbanisme et de Bâtiment, Tunis, 2035, Tunisia

[3] Université du Québec à Chicoutimi, Département des Sciences Appliquées, Saguenay, Québec, G7H 2B1, Canada

[4] University of Calgary, Department of Geoscience, Calgary, Alberta, T2N 1N4 Canada

[5] Université de Corse, CNRS UMR 6134 SPE, Département d'Hydrogéologie, Campus Grimaldi BP52, Corte, 20250, France

[6] University of Massachusetts Boston, School for the Environment, Boston, Massachusetts, 02125, USA

[7] University of Guelph, School of Engineering, Morwick G360 Groundwater Research Institute, Guelph, Ontario, N1G 2W1, Canada

[8] Helmholtz Centre for Environmental Research, Department of Catchment Hydrology, Halle, Saale, 06120, Germany

[9] University of Natural Resources and Life Sciences, Institute of Soil Physics and Rural Water Management, Vienna, 1190, Austria

Abstract (300 words max.)
Nitrate (NO_3) adversely impacts groundwater quality. In coastal salinized groundwater systems, contamination from various NO_3 inputs and complex hydrogeochemical processes make it difficult to distinguish NO_3 sources and identify potential NO_3-transformtation processes. Effective field-based NO_3 studies in coastal areas are needed to improve the understanding of NO_3 contamination dynamics in groundwater of such complex systems. This study focuses on a typical Mediterranean coastal agricultural area, located in Tunisia, experiencing substantial NO_3 contamination from multiple anthropogenic sources. Major NO_3 sources and their contributions are identified, and potential NO_3-transformation processes are described by combining multiple isotopic tracers ($\delta^{18}O_{H2O}$, $\delta^{2}H_{H2O}$, $\delta^{15}N_{NO3}$, $\delta^{18}O_{NO3}$, and $\delta^{11}B$) with the Bayesian isotope MixSIAR model. Results reveal NO_3 concentrations in groundwater above the natural baseline threshold suggesting anthropogenic influence. The isotopic composition of NO_3 indicates that manure, soil organic matter, and sewage are the potential sources of NO_3, while $\delta^{11}B$ values constrain the NO_3 contamination to manure; a finding that is supported by the MixSIAR model that reveals manure-derived NO_3 dominates over other likely sources. Nitrate derived from manure is attributed to organic fertilizers used to promote crop growth, and livestock that deposit manure directly on the ground surface. Evidence for ongoing denitrification in groundwaters is supported by an enrichment in both ^{15}N and ^{18}O in the remaining NO_3, although isotopic mass balances between the measured and the theoretical $\delta^{18}O_{NO3}$ values also suggest the occurrence of nitrification. The simultaneous occurrence of these biogeochemical processes with heterogeneous distribution across the study area reflect the complexity of interactions within the investigated coastal aquifer. The multiple isotopic tracer approach used here can identify the effect of anthropogenic activities on NO_3 sources and geochemical processes in coastal environments, which is fundamental for sustainable groundwater resources management.

Keywords
Nitrate, Aquifer, Denitrification, Nitrification, Stable isotopes, MixSIAR

1 Introduction

Nitrate (NO_3) is a ubiquitous environmental contaminant that is primarily associated with anthropogenic activities, with limited contributions from natural geological and atmospheric sources in most areas (Hendry et al., 1984; Holloway and Dahlgren, 2002; Scanlon et al., 2008). NO_3 concentrations in groundwater systems above the maximum drinking water concentration of 50 mg/L (WHO, 2017) have been observed in numerous countries with industrial agriculture. Example of aquifers with elevated groundwater NO_3 concentrations include the Mediterranean coastal aquifer of Taleza in Algeria with concentrations of up to 230 mg/L (Boumaiza et al., 2020), the Córdoba aquifers in Argentina with concentrations of up to 500 mg/L (Blarasin et al., 2014), the Weining groundwater system in China with concentrations of up to 800 mg/L (He et al., 2022), and the Noyil river basin aquifer in India in which NO_3 concentrations to up to 1,500 mg/L are reported (Jacks and Sharma, 1983). These and several other studies focussed on groundwater NO_3 contamination due to the adverse effects of NO_3 on both human and environmental health. For example, long-term consumption of excessive NO_3 in drinking water increases methemoglobinemia in infants (blue baby syndrome), and spontaneous abortion, thyroid disorders, colorectal and stomach cancer, and neural tube defects in adults (Schroeder et al., 2020; Ward et al., 2018). The discharge of NO_3 into surface water bodies causes eutrophication of freshwater and marine environments, leading to considerable reduction of aquatic life and biodiversity (Brookfield et al., 2021; Gomez Isaza et al., 2020; Yeshno et al., 2019). Incomplete denitrification of NO_3 in aquifer systems leads to the formation and release of nitrous oxide gas (N_2O), which is a powerful greenhouse gas contributing to global climate change (Sutton et al., 2011; Weeks and McMahon, 2007).

Dissolved NO_3 can also oxidize and mobilize heavy metals such as uranium and selenium (Mills et al., 2016; Moon et al., 2007).

Stable isotopic tracers have been widely used to investigate groundwater NO_3 contamination sources and processes. The stable isotopes of nitrate ($\delta^{15}N_{NO3}$ and $\delta^{18}O_{NO3}$) constitute a powerful tool not only for distinguishing NO_3 sources, but also for assessing the biogeochemical processes that govern NO_3 cycling and persistence within groundwater systems (Blarasin et al., 2020; Boumaiza et al., 2022a; Lane et al., 2020; Zendehbad et al., 2019). However, isotopic signatures of some NO_3 sources overlap, and processes such as nitrification, denitrification, and ammonia volatilization can change NO_3 concentrations and modify $\delta^{15}N_{NO3}$ and $\delta^{18}O_{NO3}$ values, masking the isotopic signature of the original NO_3 sources (Jin et al., 2015; Kendall et al., 2007). Thus, additional isotope tracers (e.g., $\delta^{11}B$, $^{87}Sr/^{86}Sr$, and $\delta^{34}S$) and statistical Bayesian models (e.g., MixSIAR) have also been used, separately or combined with the stable isotope composition of NO_3 to efficiently track NO_3 sources and quantify their relative contributions (Boumaiza et al., 2022b; Erostate et al., 2018; Kaown et al., 2023; Kruk et al., 2020). Hence, multi-isotope approaches are promising tools for identifying the NO_3 sources and evaluating the fate of NO_3 within groundwater systems.

Worldwide population growth has introduced an increased level of anthropogenic activities in rural and developing areas. Excessive use of synthetic and organic fertilizers in agricultural fields to promote crop growth contribute up to 80% of the worldwide reactive produced nitrogen and releases NO_3 to groundwater (Lasagna and De Luca, 2017; Pulido-Bosch et al., 2018). In developing urban areas, NO_3 can be transported to groundwater by wastewater discharge from inefficient private sanitation systems and sewer

systems (Boumaiza et al., 2020; Matiatos, 2016; Puig et al., 2017; Vystavna et al., 2017). The level of NO_3 contamination and its fate in groundwater systems not only depends on the type and intensity of anthropogenic activities, but also on the structure and hydrogeological characteristics of affected aquifers. In coastal aquifers, it is particular challenging to study the sources and fate of groundwater NO_3 contamination because seawater intrusion, induced by the overexploitation of groundwater and sea level rise due to climate change, can lead to mutually interacting sources and geochemical processes (Boumaiza et al., 2020; Elmeknassi et al., 2022). In addition, elevated NO_3 concentration in groundwater can fuel a number of complex geochemical reactions (Re et al., 2021; Re and Sacchi, 2017). Therefore, field-based NO_3 studies in coastal aquifers are needed to improve the understanding of NO_3 contamination in such complex hydrogeological systems.

One of the coastal groundwater systems, underlying an important economically strategic agricultural area, is the plain of Oussja-Ghar-Melah (OGM) in Tunisia. This groundwater system is located along the Mediterranean coast where groundwater resources are heavily affected by multiple anthropogenic sources of NO_3 that contribute to deteriorating groundwater quality, and is also at risk from seawater intrusion owing to overexploitation of local groundwater resources (Carrubba, 2017; Ben Ammar et al., 2016). The OGM system is subject to complex hydrogeochemical processes that can impact the fate of NO_3 within the aquifer. Moreover, the Ghar-El-Melh Lagoon (GEM Lagoon), which was designated a UNESCO-Ramsar ecological site (No.1706) in 2007 is located down hydrologic gradient from the OGM aquifer system emphasizing the international importance of the study area. Previous groundwater quality investigations within the OGM

plain chiefly focused on assessing groundwater salinization and only hypothesized potential NO_3 sources (Ben Ammar et al., 2016; Bouzourra et al., 2015). A detailed investigation of groundwater NO_3 contamination and potential transformation processes affecting NO_3 in the aquifer underlying the OGM plain have not yet been conducted. Therefore, the main objectives of this study are: (i) to identify the dominant anthropogenic sources of NO_3 and distinguish potential NO_3 transformation processes within the OGM groundwater system by combining multiple stable isotope tracers ($\delta^{18}O_{H2O}$, $\delta^{2}H_{H2O}$, $\delta^{15}N_{NO3}$, $\delta^{18}O_{NO3}$, and $\delta^{11}B$); and (ii) quantify the contributions of different NO_3 sources by using a Bayesian isotope mixing model (MixSIAR). Ultimately, the outcomes of this study will help local groundwater managers to develop sustainable environmental management strategies for the OGM plain; and inform future studies of the many Mediterranean coastal systems with similar environmental stresses.

2 Description of the study area

2.1 Geographic location and climate

The study area of the OGM is a coastal agricultural plain located at the border of the Provinces of Bizerte and Ariana in northeastern Tunisia (Figure 1). The study area is surrounded from the southwest to the northeast by a series of discontinuous mountains (i.e., Menzel Ghoul, Kechabta, and Nadhour) varying in altitude from 300 to 400 m above sea level. Towards the south, the OGM plain is an open and flat valley system belonging to the Medjerda paleodelta. The northeast-southeast boundary of the study area constitutes the GEM Lagoon, which is connected to the Mediterranean Sea (Figure 1). The study area covers a surface of about 60 km^2, with topography characterized by a slight downslope from the hinterland in the southwest towards the Mediterranean Sea in the east and

northeast (Ben Ammar et al., 2016). Several large rural villages are located in the study area including Ghar-El-Melh to the northeast, Zouaouine and Gournata to the southwest, and Oussja within the center of the plain. Between these population centers are many smaller rural communities.

The climate of the study area is subhumid Mediterranean with two distinct periods: (i) a wet period, occurring from October to April, with a monthly average temperature of 11 °C; and (ii) a dry period, occurring from May to September, with a monthly average temperature of 27 °C (Ben Ammar et al., 2016). The OGM region captures an average annual precipitation amount of about 500 mm with 90% occurring during the wet period (Ben Ammar et al., 2016). The assessed mean annual potential evapotranspiration is estimated to be ~1,350 mm, clearly indicating a deficient annual water budget for the study area. Nevertheless, the excess of meteoric precipitation during the wet period provides potential for aquifer recharge (Ben Ammar et al., 2016; Bouzourra et al., 2015).

2.2 Geology

The study area belongs to a tectonic depression that filled with clastic sediments following a major Mio-Pliocene subsidence. This depression was previously invaded by a postglacial marine transgression, developing a marine paleoenvironment; after which the depression gradually infilled with fluvial deposits (i.e., sand, silt, and clay) initially transported by the Medjerda River (Burrolet and Dumon, 1952; Pimienta, 1959). The study area thus evolved from a marine lagoon into a coastal evaporitic basin, in which the GEM Lagoon represents the current remnant of the Utique paleoshoreline (Bouzourra et al., 2015). The aquifer under the plain of OGM is comprised of granular material provided by the Late-Pliocene/Quaternary deposition.

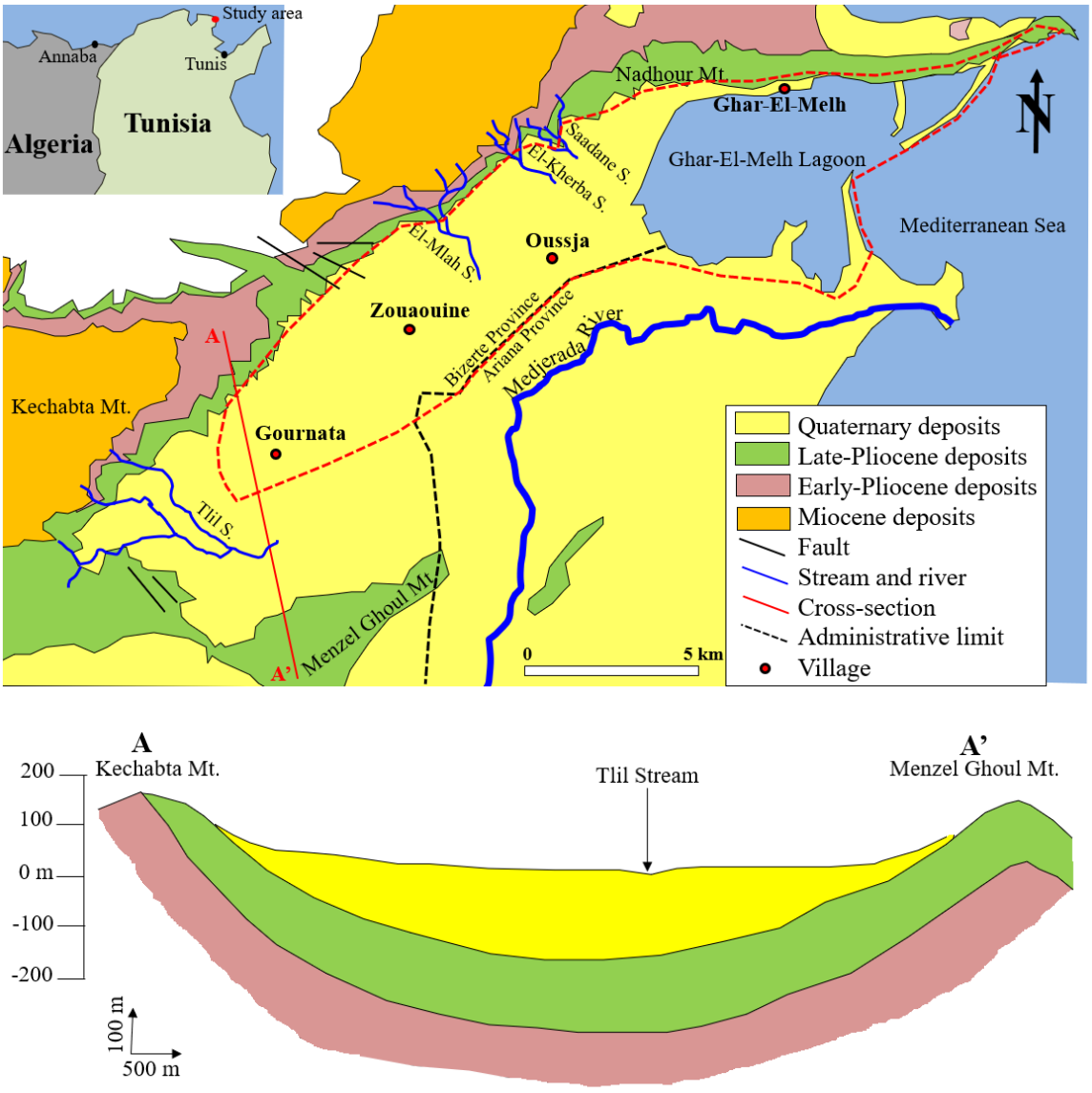

Figure 1. Simplified geology of surface deposits over the plain of OGM region, and schematic cross-section AA' through the study area (adapted from Burrolet and Dumon, 1952; Melki et al., 2011). In dashed red is the approximate limit of the study area. Only the permanent streams are indicated in this figure.

Geophysical Seismic reflection investigations demonstrated that the thickness of the Plio-Quaternary deposits varies from 300 m at the southwest sector of the study area to >600 m in the northeast (Melki et al., 2011). The granular Plio-Quaternary deposits unconformably rest on Mio-Pliocene sequence that consists of clay, marl, and gypsum,

which outcrops in the surrounding mountains (Figure 1). Miocene rocks are covered in some places by clay material attributed to the Early Pliocene (Burrolet and Dumon, 1952; Chelbi et al., 1995). A ~300 m thick Late-Pliocene formation (Porto Farina formation) overlies the impervious Miocene and Early Pliocene units, and is mainly composed of sand and sandstone with clays intercalations (Burrolet and Dumon, 1952; Melki et al., 2011).

2.3 Hydrogeological background

The OGM plain overlies an unconfined heterogeneous granular aquifer with a thickness of up to 100 m (Ben Ammar et al., 2016). This aquifer is mainly recharged by direct precipitation, runoff from the surrounding mountains, and by several permanent streams including the Saadane, El-Kherba, and El-Melah streams in the north, and Tlil stream in the southwest, all of which are sourced from the surrounding mountains. These streams drain small catchment areas ranging from 6 to 17 km^2 (Saadaoui, 1983). The water table in the aquifer varies between 2 and 24 m depth below the ground surface, and groundwater generally flows northeastward towards the GEM Lagoon and Mediterranean Sea (Ben Ammar et al., 2016). The chemistry of groundwater within the OGM aquifer is dominated by chloride-water type, i.e., (Na, Ca)-Cl-rich, which are hypothesized to reflect multiple hydrogeochemical processes including dissolution/precipitation of carbonate minerals, dissolution of gypsum and halite, and cation exchange (Ben Ammar et al., 2016; Bouzourra et al., 2015). Groundwater salinization is thought to be the result of seawater intrusion and the deposition of seawater aerosols flushing into the subsurface (Ben Ammar et al., 2016).

The OGM aquifer system is considered to be vulnerable to the contamination with three levels based on the DRASTIC index (Ouerghi, 2021). These are as follows: (i) a zone with low vulnerability to contamination, representing 28% of the study area, and located

in the northeastern portion of the study area proximal to Ghar-El-Melh village; (ii) a second zone, occupying the center of the study area (45%) close to Oussja and Zouaouine villages with an average vulnerability level; and (iii) a third zone with very high vulnerability level (27%) located in the southwestern part of the study area (around Gournata).

2.4 Land use and anthropogenic contamination

The earliest first settlements in the study area include the large villages of Ghar-El-Melh in the northeast, Zouaouine and Gournata in the southwest, and Oussja in the center of the plain (Figure 1). Subsequently, several small rural communities developed throughout the study area with an approximate combined population of 19,000 permanent inhabitants. The rural communities in the study area are connected to a potable water supply via a pipeline-system provided by SONEDE (*Société Nationale d'Exploitation et de Distribution des Eaux*). However, only 60% of the rural sectors, including the large villages of Ghar-El-Melh and Oussaja, are connected to a sewage network, which has only operated since 2010. Before 2010, all the communities used private septic tank systems.

Despite increased urbanization across the study area, agricultural fields still dominate the land use (~80%). Agricultural activities (i.e., production of various vegetables in open agricultural fields) are supported by irrigation using surface waters from three following sources: (i) the Medjerda River located at the south of the study area, (ii) an artificial drainage network operated since 1990 over the central part of the study area, and (iii) a series of small dams installed at the edges of the surrounding mountains to the north. In addition, there is a large number of shallow hand-dug wells (~1,500 wells) in the study area that are used to obtain groundwater for irrigating the agricultural fields (Ben Ammar et al., 2016; Bouzourra et al., 2015).

The effect of both agriculture and urban development resulted in a deterioration of groundwater quality with regards to nitrate concentrations (Bouzourra et al., 2015; Ouerghi, 2021). Reported groundwater NO_3 concentrations ranged from 5 to 150 mg/L, with elevated NO_3 concentrations coinciding with locations of intense urbanization and agricultural activities (Ben Ammar et al., 2016; Bouzourra et al., 2015). These researchers suggested that organic/synthetic fertilizers used for agriculture, livestock (i.e., cattle for dairy and meat production) manure, and septic tanks constituted the major sources of NO_3 (Ben Ammar et al., 2016; Bouzourra et al., 2015; Carrubba, 2014). However, clear evidence demonstrating the sources of the groundwater NO_3 contamination has not been reported. Increasing demand for irrigation water has generated substantial groundwater exploitation reaching 13 million cubic meters per year (in 2009), which is roughly 2-fold higher than the annual aquifer recharge (Ben Ammar et al., 2016; Bouzourra et al., 2015; MAT, 2006). Hence, overexploitation of groundwater led to drop in elevation of the water table within the OGM aquifer that has subsequently supported seawater intrusion in some locations, along groundwater salinization to as much as 3,000 mg/L for total dissolved solids (Ayache et al., 2009; Bouchouicha, 2004; Bouzourra et al., 2015).

3 Material and methods

3.1 Sampling network and protocol

A comprehensive water sampling campaign was carried out between October 19 and November 2, 2022. The sampling campaign included 21 groundwater samples collected over the entire study area and 2 surface water samples, one each collected from the GEM Lagoon and the Mediterranean Sea (Figure 2). Groundwater samples were collected from shallow irrigation wells having 2-3 m diameters, with a static groundwater depth of 2-20

m below the ground surface. Prior to sampling, stagnant groundwater present in the wells was purged using a pumping system. During pumping the physico-chemical parameters (temperature (T), pH, total dissolved solids (TDS), electrical conductivity (EC), and dissolved oxygen (DO)) of the pumped groundwater were monitored using a calibrated portable multiparameter probe (Lange sensION 156 Hach Instrument), until stabilized within ±10%. Groundwater was then collected at the discharge pipe of the pumping system.

During fieldwork, the water samples for major ion analyses were filtered using 0.45-μm nitrocellulose membrane filters attached to 100-mL luer-lock syringe samplers, before being poured in two separate 40-mL amber bottles. Cation samples were acidified to pH <2 by adding 2-3 drops of ultrapure nitric acid (HNO_3) to prevent major cation precipitation or adsorption during storage. The samples for δ^2H_{H2O} and $\delta^{18}O_{H2O}$ analyses were collected in 25-mL amber bottles, whereas those for $\delta^{15}N_{NO3}/\delta^{18}O_{NO3}$, and $\delta^{11}B$ analyses were filtered into 50-mL and 250-mL polyethylene bottles, respectively. All water samples were collected in bottles without headspace and closed with caps containing Teflon septa parafilm to prevent evaporation. All water samples were temporarily stored in a portable cooler before being transferred further to a refrigerator for storage at 4°C at the completion of the fieldwork day until analysis. The samples collected for isotopic analysis of NO_3 were frozen to avoid variations caused by biological processes until the targeted isotopic analyses were performed in the laboratory.

3.2 Laboratory chemical and stable isotope analyses

Chemical analyses (HCO_3^-, Br^-, NO_3^-, Cl^-, K^+, Mg^{2+}, NH_4^+, Na^+, Ca^{2+} and SO_4^{2-}) were performed at the Laboratory for Inorganic and Organic Chemistry of the Technical University of Darmstadt (Germany). HCO_3 concentrations were determined using

Alkalinity Checker® (HI775, Hanna Instruments, Woonsocket, USA), whereas the other ion concentrations were determined using a Metrohm 882 Compact Ion Chromatograph plus equipped with a Metrosep A Supp 5-250 column for anions and a Metrosep C 4-250 column for cations (Metrohm, Herisau, Switzerland). The water stable isotope ($\delta^{2}H_{H2O}$ and $\delta^{18}O_{H2O}$) analyses were completed at the Laboratory of the Institute of Soil Physics and Rural Water Management in Vienna (Austria). These isotopic values were measured using a laser-based isotope analyzer (Picarro L2140-*i*) according to the analytical scheme recommended by the International Atomic Energy Agency (IAEA) (Penna et al., 2010). Nitrate stable isotope ($\delta^{15}N_{NO3}$ and $\delta^{18}O_{NO3}$) analyses were completed at the Helmholtz Center for Environmental Research in Halle/Saale (Germany), using the denitrifier method with bacteria strains of *Pseudomonas chlororaphis* (ATCC #13985 equal to DSM-6698) according to the protocols recommended by Casciotti et al. (2002) and Sigman et al. (2001).

Boron (B) concentrations and $\delta^{11}B$ values in water samples were both analyzed at the Isotope Science Laboratory of the University of Calgary (Alberta, Canada). Concentrations of dissolved boron in groundwater were measured using a Varian 725 inductively coupled plasma-optical emission spectrometer (ICP-OES) with a measurement uncertainty ±2%, whereas $\delta^{11}B$ values were measured using a Neptune Multi-Collector Inductively Coupled Plasma Mass Spectrometer (MC-ICP-MS) (Thermo Scientific) according to the analytical schemes recommended by Guerrot et al. (2011) and Gaillardet et al. (2001) depending on the B concentration of the samples. The isotope values, expressed in per mil (‰) using delta (δ) notation, were calculated using Equation 1, in which R_{sample} and $R_{standard}$ are the sample and the international reference standard values of the heavier to the lighter isotope, respectively (i.e., $^{2}H/^{1}H$, $^{18}O/^{16}O$, $^{15}N/^{14}N$, or $^{11}B/^{10}B$).

$$\delta = \frac{R_{sample} - R_{standard}}{R_{standard}} \quad (1)$$

The international reference standards relative to which the sample isotopic values are reported are the Vienna Mean Standard Ocean Water (VSMOW) for $\delta^{2}H_{H2O}$, $\delta^{18}O_{H2O}$ and $\delta^{18}O_{NO3}$, and atmospheric nitrogen (AIR) for $\delta^{15}N_{NO3}$. The precision of the analytical instrument was generally better than ±0.3‰ for $\delta^{2}H_{H2O}$ and ±0.1‰ for $\delta^{18}O_{H2O}$, whereas the reproducibility for the $\delta^{15}N_{NO3}$ and the $\delta^{18}O_{NO3}$ measurements were ±0.6‰ and ±0.4‰, respectively. The isotope measurements of $\delta^{11}B$ had a mean precision of ±2‰, which was determined following a replicate analysis of standards and samples. In the present study, the $\delta^{18}O_{H2O}$ and $\delta^{2}H_{H2O}$ values are interpreted according to the Global Meteoric Water Line (GMWL) (Craig, 1961) and the Western Mediterranean Meteoric Water Line (WMMWL) (Celle, 2000).

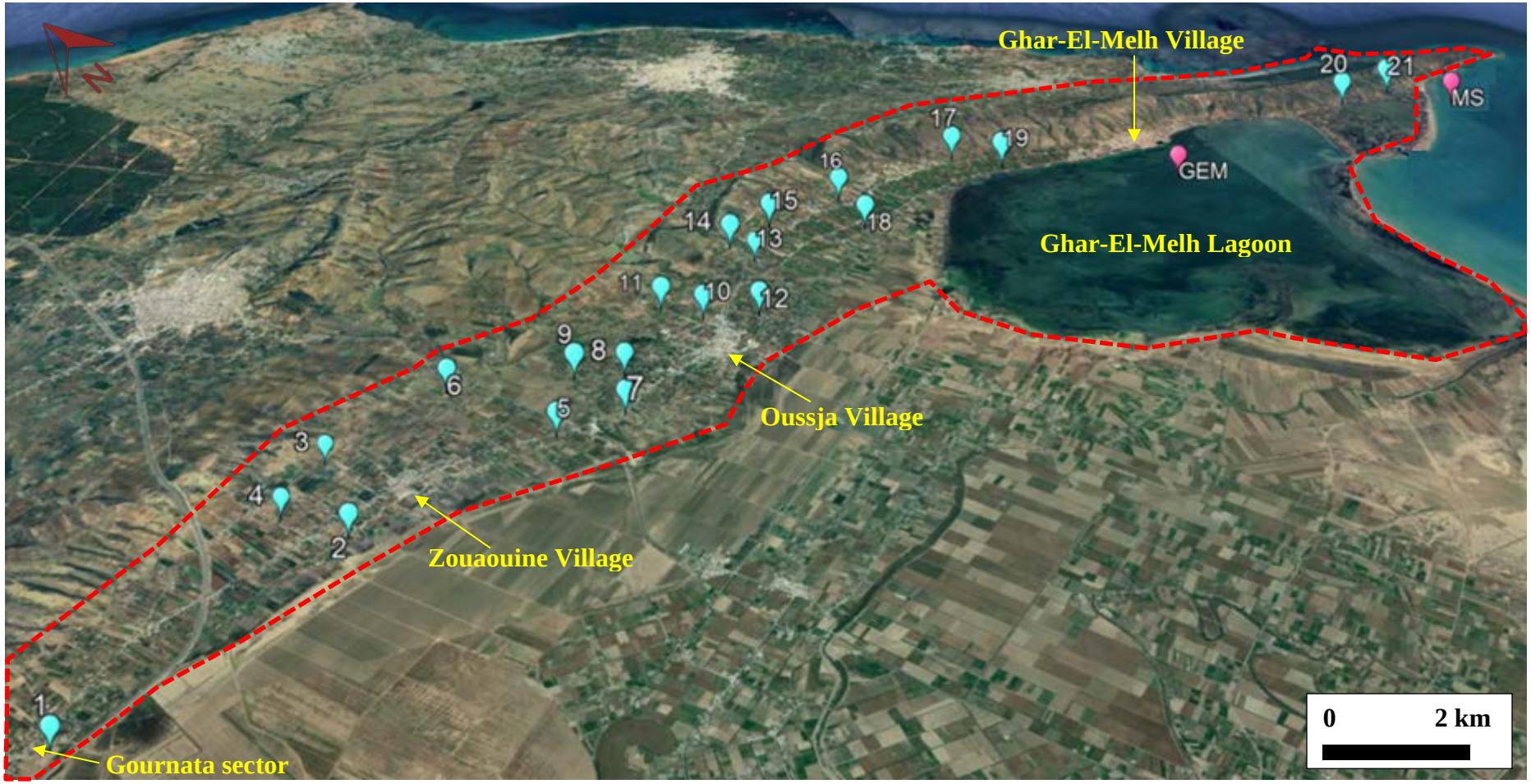

Figure 2. Perspective overview of study area (Google Earth) with location of groundwater samples and surface water samples collected over the study area. Groundwater sampling sites are indicated with numbers 1 to 21, whereas surface water samples are GEM (Ghar-El-Melh Lagoon) and MS (Mediterranean Sea). The red dashed line is the approximate limit of the study area including the GEM Lagoon.

3.3 Nitrate sources determination, apportionment, and transformation

To identify the predominant NO_3 sources in water samples, the $\delta^{15}N_{NO3}$ versus $\delta^{18}O_{NO3}$ diagram (Kendall, 1998) is used. This diagram provides zones of isotopic compositions that correspond to specific sources of NO_3, which include atmospheric precipitation (AP), NO_3-based synthetic fertilizers (NOF), sewage and manure (S&M), NO_3 that is formed from nitrification of NH_4-fertilizers (NHF), or soil organic nitrogen (SON). To identify the occurrence of nitrification, an isotopic mass balance ($\Delta\delta^{18}O_{NO3}$) between the measured $\delta^{18}O_{NO3}$ and the theoretical $\delta^{18}O_{NO3}$ is calculated. The theoretical $\delta^{18}O_{NO3}$ is evaluated by using Equation 2 (Aravena and Mayer, 2010), where $\delta^{18}O_{H2O}$ represents the measured oxygen groundwater stable isotope ratio and $\delta^{18}O_{O2}$ is the isotopic ratio of atmospheric oxygen assumed in equilibrium with a constant value of +23.5‰ (Aravena and Mayer, 2010; Blarasin et al., 2020; Moore et al., 2006). The contribution of NO_3 derived from nitrification process is calculated as a portion of the theoretical $\delta^{18}O_{NO3}$ to the measured $\delta^{18}O_{NO3}$ (Torres-Martínez et al., 2021).

$$\delta^{18}O_{NO3\ (theoretical)} = \left(\frac{2}{3}\ \delta^{18}O_{H2O}\right) + \left(\frac{1}{3}\ \delta^{18}O_{O2}\right) \quad (2)$$

Other diagrams and a Bayesian isotope model are used to distinguish between sewage and manure sources affecting groundwater contamination. Here, a diagram comparing B concentrations and $\delta^{11}B$ values and a plot of $\delta^{15}N_{NO3}$ versus $\delta^{11}B$ values are used. Both of these diagrams provide distinct zones for manure and sewage, thus providing a means to differentiate between manure and sewage sources (Komor, 1997; Puig et al., 2017; Vengosh et al., 1994). The MixSIAR model (Parnell et al., 2010) is used to quantify the proportional contributions of the identified NO_3 sources in the groundwater system.

More detail on the MixSIAR model development can be found in Stock et al. (2018). The inputs for the MixSIAR model are the $\delta^{15}N_{NO3}$ and $\delta^{11}B$ values measured in groundwater samples and the different $\delta^{15}N_{NO3}$ and $\delta^{11}B$ end-member isotopic values of the sources of nitrate. Here, the $\delta^{15}N_{NO3}$ and $\delta^{11}B$ end-members are adopted from Kaown et al. (2023), who investigated NO_3 contamination in an area with comparable anthropogenic sources.

4 Results

4.1 Chemical and isotopic composition of water

The chemical and isotopic results for the groundwater samples as well as the surface water samples collected from the GEM Lagoon and the Mediterranean Sea are listed in the Supplementary Table S1. Groundwater exibits TDS values ranging from 630 to 4,280 mg/L reflecting the existance of fresh to brackish waters within the OGM aquifer. The isotopic compositions of the groundwater samples range from −5.7‰ to −4.1‰ for $\delta^{18}O_{H2O}$ and from −32.1‰ to −24.3‰ for $\delta^{2}H_{H2O}$, with d-excess values ranging from +8 to +15‰ with a median value of +12‰. The GEM Lagoon sample has the highest $\delta^{18}O_{H2O}$ and $\delta^{2}H_{H2O}$ values (+1.4‰ and +9.7‰, respectively) and is comparable to the sample from the Mediterranean Sea (+1.3‰ and +9.5‰, respectively). These saline surface water samples, with TDS ranging from 33,000 to 39,000 mg/L, are enriched in ^{2}H and ^{18}O compared to groundwater samples and exhibit a low d-excess value (−1.1‰).

4.2 Distribution of nitrate across the study area

NO_3 concentrations in groundwater samples range from 4 to 489 mg/L, with an average of 132 mg/L (n=21). Surface water samples from the GEM Lagoon and the Mediterranean Sea have NO_3 concentrations of 87 and 104 mg/L, respectively (Supplementary Table S1). The distribution of NO_3 concentrations throughout the study area (Figure 3) shows two

groundwater samples (#1 and #21) with NO_3 concentrations <10 mg/L located at the boundaries of the study area. Sample #1 is from the southwestern portion of the study area (sector of Gournata), whereas sample #21 is from the northeastern part of the study area (sector of Ghar-El-Melh village). In 2010, NO_3 concentrations in groundwater from these sectors were measured at 43 and 38 mg/L, respectively (Ben Ammar et al., 2016). In 2010, groundwater samples most affected by NO_3 were observed in the sectors of Oussja and Zouaouine, with NO_3 concentrations ranging from 50 to 136 mg/L (Ben Ammar et al., 2016). This is consistent with observations from the present study, as elevated NO_3 concentrations are observed in these same sectors, but with a maximum of 378 mg/L (sample #8), i.e., two times higher than the NO_3 concentration measured in 2010. In this area, there is a high number of wells supplying groundwater with elevated NO_3 concentrations >150 mg/L (Figure 3), suggesting the existence of major and permanent sources of NO_3 affecting groundwater. The highest NO_3 concentration (489 mg/L) is observed in the groundwater sample #17 collected between Ghar-El-Melh and Oussja village at a location dominated by agricultural activities and surrounded by multiple individual residences.

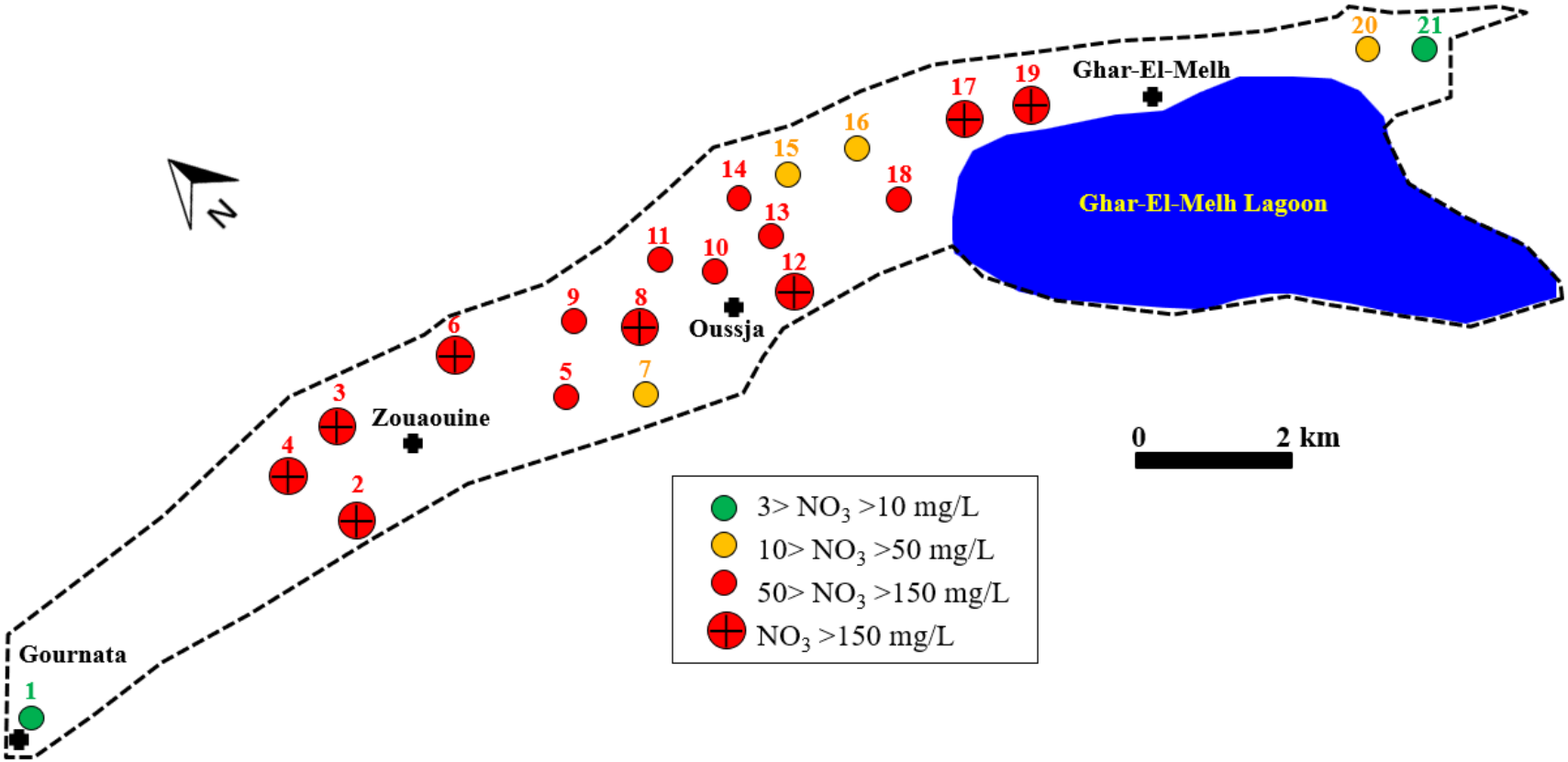

Figure 3. Spatial distribution of NO_3 concentrations in groundwater throughout the study area.

4.3 Isotopic compositions of nitrate and boron and sources of nitrate

The $\delta^{15}N_{NO3}$ values in groundwater range from +4.7 to +13.7‰ with a median value of +7.1‰, and $\delta^{18}O_{NO3}$ values vary between +4.1 and +15.6‰ with a median value of +7.5‰ (Supplementary Table S1). These median values are consistent with the range (4.9-11‰ and 5.7-12‰, respectively) of NO_3-isotopic compositions observed in other North-African coastal studies (Boumaiza et al., 2022a, 2022b, 2020; Re et al., 2021). The measured $\delta^{11}B$ values in groundwater samples range from +12.4 to +42.9‰, whereas in the GEM Lagoon and Mediterranean Sea they are +42.3 and +41.4‰, respectively (Supplementary Table S1). All groundwater samples (*n*=20) plot within the manure and sewage field of the Kendal diagram (Figure 4a), suggesting that manure and human wastewater are the main sources of NO_3 to local groundwater. However, 14 samples have NO_3 isotopic compositions that overlap with NO_3 from soil-derived nitrogen (Figure 4a). Boron isotope data indicate that manure is the principal source of NO_3 for most of the groundwater samples (18 out of 20) as well as the GEM Lagoon and the Mediterranean Sea (Figures 4b, c). The two remaining groundwater samples (#6 and #11) likely derive their NO_3 from mineral fertilizer (Figure 4b, c).

In the MixSIAR model, four NO_3 sources are selected including manure (M), sewage (S), soil organic nitrogen (SON) (Figure 4a) and mineral fertilizer (NO_3-based fertilizers: NOF (Figure 4b, c). The assigned $\delta^{15}N_{NO3}$ end-members are 15.3±0.1‰ for M, 14.3±2.0‰ for S, −0.6±4.1‰ for SON, and 0.9±2.0‰ for NOF, whereas the $\delta^{11}B$ end-members are 33.1±2.1‰ for M, 5.4±2.7‰ for S, −2.6±1.9‰ for SON, and 2.0±1.0‰ for NOF (Kaown et al., 2023). MixSIAR results reveal that manure is the primary source of NO_3 (60.4%), followed by NOF (19.1%), SON (16.1%), and sewage (4.3%) (Figure 4d).

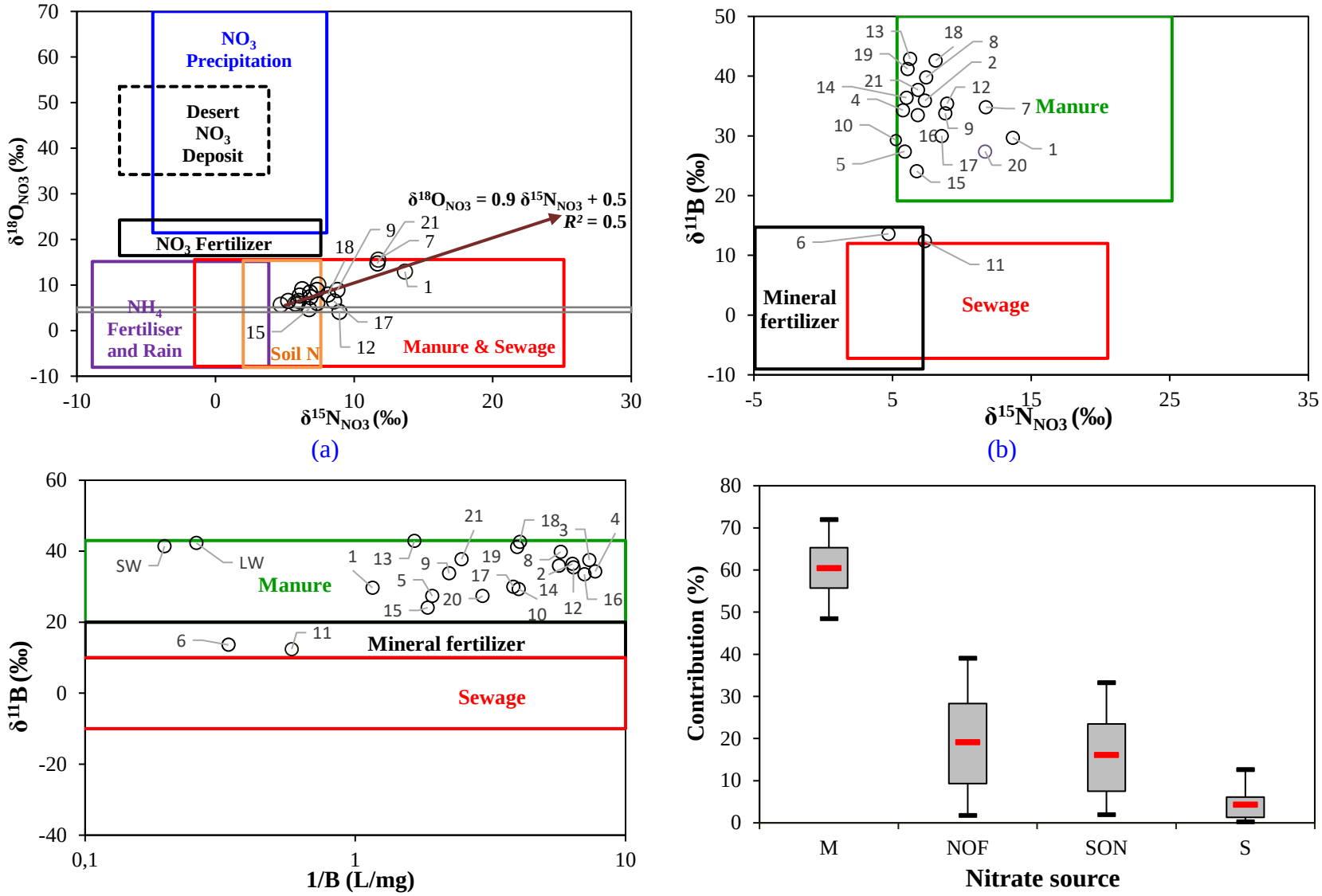

Figure 4. (a) Plot of $\delta^{15}N_{NO3}$ versus $\delta^{18}O_{NO3}$ values on Kendall diagram; (b) Plot of $\delta^{15}N_{NO3}$ versus $\delta^{11}B$ values; (c) Plot of B concentrations versus $\delta^{11}B$ values; and (d) apportionment of NO_3 sources based on the MixSIAR model (M: manure, NOF: NO_3-based fertilizers, SON: soil organic nitrogen, S: sewage). Boxplots illustrate the 25th, 50th, and 75th percentiles, while the whiskers indicate 5th and 95th percentiles.

5 Discussion

5.1 Water origin and influencing processes

The isotopic compositions of the groundwater samples are comparable to those from other studies undertaken on North-African Mediterranean coastal aquifers (Boumaiza et al., 2022a, 2020; Chafouq et al., 2018; Elmeknassi et al., 2022; Moussaoui et al., 2023). Furthermore, the groundwater isotopic compositions are comparable to the local weighted isotopic mean of wet season precipitation ($\delta^{18}O_{H2O}$ = −4.7‰, and $\delta^{2}H_{H2O}$ = −26.1‰) (Ben Ammar et al., 2020), suggesting that the OGM aquifer is mainly recharged by meteoric precipitation during the wet season, consistent with the fact that most precipitation occurs during the wet period from October to April in the study region. Most of $\delta^{18}O_{H2O}$ and $\delta^{2}H_{H2O}$ values plot along the GMWL (Craig, 1961) and the WMMWL (Celle, 2000) in Figure 5, suggesting that groundwater is mainly recharged through direct infiltration of meteoric recharge. The hydrogeological characteristics of the study area, i.e., an unconfined granular aquifer with a transmissivity of about 1-9×10^{-4} m^2/s (Ben Ammar et al., 2016), are supportive of this conclusion.

Since substantial agricultural and irrigation activities occur across the study area, hydrogen and oxygen isotope fractionation affecting infiltrating water due to evaporation is expected if irrigation water-return flow is a significant source of recharge (Clark and Fritz, 1997; Harvey and Sibray, 2001; Mahlknecht et al., 2008). Some groundwater samples (#5, #15, #16, and #17) exhibit d-excess values <10‰, which could indicate some evaporation influence, but most samples (*n* = 17/21) have d-excess values >10‰, which is too high for significant evaporation effects (Santoni et al., 2018). The $\delta^{18}O_{H2O}$ values display little variability (with values of −4.9±0.5‰) across the groundwater samples with

a wide range of measured TDS values (629-4,280 mg/L) (Supplementary Figure S1a). This suggests that evaporation is not the dominant process that increases groundwater salinity (Jia et al., 2017; Torres-Martínez et al., 2021). Rather, the increase in TDS appears to be caused by mixing with seawater. This notion is supported by the fact that the groundwater isotopic data plot along a line directed towards the isotopic composition of Mediterranean Sea and GEM Lagoon water (Figure 5). The water samples collected from the GEM Lagoon and from the Mediterranean Sea plot below the WMMWL and exhibit a low d-excess value (−1.1‰) (Figure 5; Supplementary Table S1). These observations indicate heavy isotope enrichment due to evaporative isotope fractionation effects and indicates the source water for the GEM Lagoon is from the Mediterranean Sea.

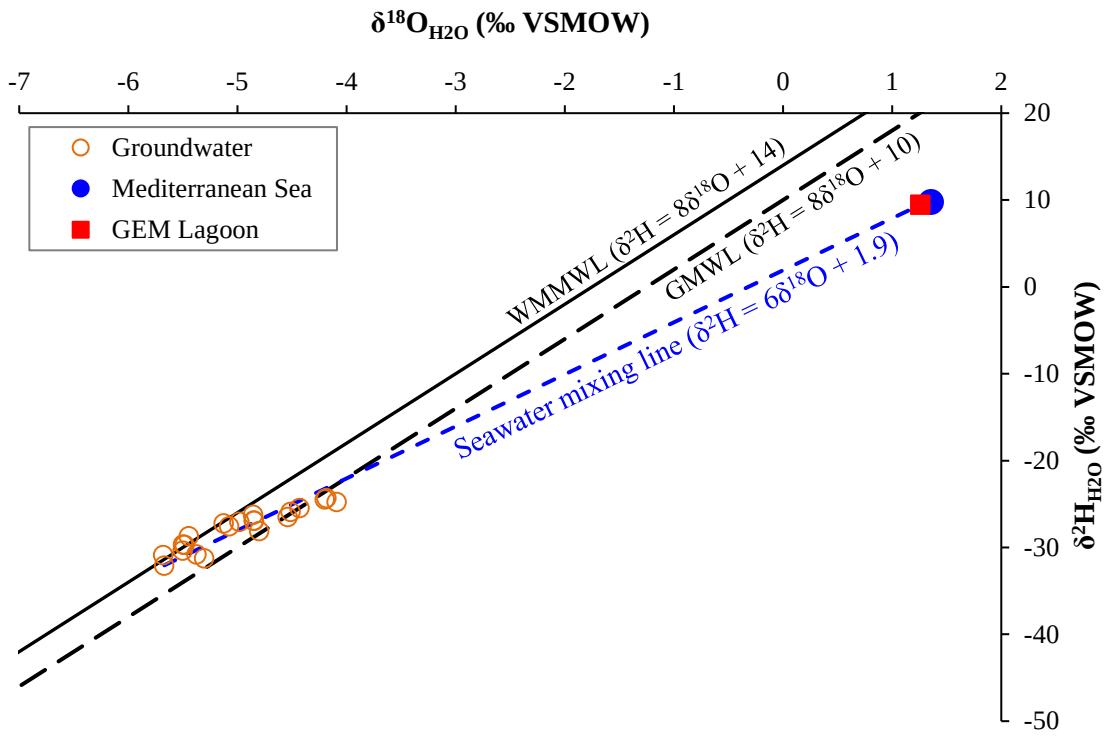

Figure 5. Distribution of isotopic values of water samples including groundwaters, surface water from GEM Lagoon, and surface water from the Mediterranean Sea.

5.2 Nitrate origin in groundwater system

All the measured NO_3 concentrations in the groundwater samples exceed the natural baseline threshold value of 3 mg/L (Ogrinc et al., 2019; Zendehbad et al., 2019), suggesting anthropogenic contamination in the study area, with 71% of the NO_3 concentrations in groundwater exceeding the drinking water limit. The finding from diagnostic plots (Figure 4) that manure is the dominant source of the elevated NO_3 concentrations in these groundwaters is consistent with land use within the OGM plain. Specifically, the OGM plain is a traditional agricultural area with a long history of intense fertilization/cultivation/irrigation activities. Manure-derived NO_3 in the groundwater appears to be linked to the excessive use of animal manure, which is applied as fertilizer for crops in agricultural areas, as well as manure that accumulates on the ground surface at local animal farms (Ben Ammar et al., 2016; Carrubba, 2017). Furthermore, these agricultural activities result in the accumulation of soil organic nitrogen and the subsequent formation of NO_3 from manure-based fertilizers infiltrating into the groundwaters as revealed by the quantified NO_3 contributions from manure, NOF, and SON (Figure 4d). Infiltrating rainwater and irrigation return flow contribute to the leaching of NO_3 from fertilizers and their by-products, which is then transported into the underlying groundwater system (Malki et al., 2017; Zhang et al., 2014). Leaching fertilizers is supported by the moderate positive correlation (R^2=0.5) between groundwater NO_3 concentrations and $\delta^{18}O_{H2O}$ values for groundwater samples (Supplementary Figure S1b) with manure-derived contributions (60.4%) dominating over synthetic fertilizers (19.1%) according to the MixSIAR model. However, the contribution of synthetic fertilizers to NO_3 in groundwater

is relatively high compared to other Mediterranean agricultural areas, where contributions range between 8 and 15% (Boumaiza et al., 2022a, 2022b).

Elevated NO_3 concentrations (>150 mg/L, Figure 3) are observed in groundwater down hydrogeologic gradient of the rural communities, suggesting that the minor sewage contribution revealed by MixSIAR model is potentially from residences using inadequate private sanitation systems (Ben Ammar et al., 2016; Carrubba, 2014). While efficient private sanitation systems have a closed septic tank connected to a seepage distribution field (MDDELCC, 2015), many private sanitations systems in North-Africa rely on a unique open-bottom tank through which human waste can directly seep into the subsurface and reach groundwater (Boumaiza et al., 2021, 2019). Consequently, sewage-derived NO_3 in groundwater is likely from direct wastewater discharge or leakage from inadequate private sanitation systems. Even though ~40% of private homes in the OGM area rely on the use of private sanitation systems (Ben Ammar et al., 2016), the sewage contribution quantified by MixSIAR is low (4%), whereas $\delta^{11}B$ values indicate negligible sewage contributions towards NO_3 in the OGM groundwater system. It is likely that mixing of sewage-sourced and manure-sourced NO_3 occurs within the OGM groundwater system although the isotope data demonstrate the manure is chief source of NO_3 contamination. It is also important to note that the present study relies on MixSIAR isotopic end-member values from another similar cases study (Kaown et al., 2023), and therefore analysing the isotopic end-member compositions of local sources is necessary to refine our estimates and thus improve characterization of the local NO_3 sources.

The elevated NO_3 concentrations in samples collected locally from the GEM Lagoon and the Mediterranean Sea, combined with $\delta^{11}B$-evidence of manure influence,

may reflect organic manure used as part of the Ramli agricultural systems distributed across the banks of GEM Lagoon (Aissaoui, 2020). Also, it cannot be rule out that there are potential groundwater-surface water interactions that allow transport of NO_3 from the OGM groundwater system into the GEM Lagoon and the Mediterranean Sea (e.g., submarine groundwater discharge). NO_3 transport from the OGM groundwater system to the GEM Lagoon is further supported by groundwater flow as it is directed from the OGM aquifer towards the GEM Lagoon (Supplementary Figure S2).

5.3 Nitrate transformation processes in the OGM groundwater system

The most common nitrogen transformation processes include nitrification and denitrification, which are biogeochemical processes mostly inherent to shallow groundwater systems that are dependent on redox conditions (Gutiérrez et al., 2018). During the denitrification process, ^{15}N and ^{18}O become progressively enriched in the remaining NO_3, and $\delta^{15}N_{NO3}$ and $\delta^{18}O_{NO3}$ values in the remaining NO_3 pool increase as the NO_3 concentration decreases (Kendall et al., 2007). Hence, the dual isotope plot of $\delta^{15}N_{NO3}$ versus $\delta^{18}O_{NO3}$ reveals that if microbial denitrification occurs in groundwater, it will manifest as a positive slope of 0.5 or higher on the trendline between $\delta^{15}N_{NO3}$ and $\delta^{18}O_{NO3}$ values of NO_3 (Böttcher et al., 1990; Chen and MacQuarrie, 2005; Fukada et al., 2004; Singleton et al., 2007). In Figure 4a, the plot of $\delta^{15}N_{NO3}$ against $\delta^{18}O_{NO3}$ values shows a positive slope of 0.9 suggesting that denitrification appears to occur in the OGM groundwater system. However, denitrification cannot be the only biogeochemical processes responsible for decreases in NO_3 concentrations because the correlation between $\delta^{15}N_{NO3}$ values and NO_3 concentrations is weak (R^2 = 0.03, Supplementary Figure S1c). Nevertheless, because most groundwater samples (n = 19/20) have positive $\Delta\delta^{18}O_{NO3}$

values ranging from +1.2 to +10.7‰ (Supplementary Table S1), the $\delta^{18}O_{NO3}$ data are also consistent with denitrification occurring within the OGM groundwater system. On the other hand, because some of groundwater samples plot within/near the expected theoretical interval of $\delta^{18}O_{NO3}$ that ranges from 4.0 to 5.1‰ (Figure 4a; Supplementary Table S1), nitrification must also be occurring within the OGM groundwater system.

Dissolved oxygen measured in groundwater samples from the study area ranges from undetected to 7 mg/L (Supplementary Table S1). Hence, the DO concentrations in groundwater samples with values >4 mg/L would tend to limit denitrification (Nikolenko et al., 2018), which is not expected in highly oxygenated groundwaters. However, denitrification could occur at anoxic sub-regions along the flow-paths and not necessarily at the sampling locations. The plot of DO concentrations against pH values (Supplementary Figure S1d) shows that groundwater samples #7, #8, #10, #12, and #13 (with measured DO concentrations ranging from 0.2 to 3.3 mg/L) fall into the optimal denitrification zone, suggesting that these samples are undergoing denitrification potentially under partially oxidized conditions. In Figure S1e, groundwater samples #2, #9, #14, #16, and #21 plot within the optimum nitrification zone suggesting NO_3 may reflect nitrification whereby potential partial nitrification contributed an estimated of 76, 57, 71, 50, and 57%, respectively, (Supplementary Table S1). The $\Delta\delta^{18}O_{NO3}$ values for samples #1 (8.9‰), #7 (10.8‰), and #21 (10.3‰) are high due to elevated measured $\delta^{18}O_{NO3}$ values, which range from 11.7 to 13.7‰. This suggests that denitrification is taking place in the aquifer yielding groundwater at wells #1, #7, and #21. However, sample #21 also falls within the optimal nitrification zone due to its elevated DO concentration (Supplementary Figure S1d), even though it has similar NO_3 isotopic values to that of sample #7 (Figure 4a). All the above

observations support that both denitrification and nitrification are important geochemical processes of the nitrogen cycle within the OGM groundwater system.

6 Conclusion

The present study combined multiple environmental isotopic tracers ($\delta^{18}O_{H2O}$, $\delta^{2}H_{H2O}$, $\delta^{15}N_{NO3}$, $\delta^{18}O_{NO3}$, and $\delta^{11}B$) with a Bayesian isotope MixSIAR model to distinguish NO_3 sources and their relative contributions; and to identify potential NO_3-transformation processes in a coastal aquifer located in Tunisia. All collected groundwater samples from the Mediterranean OGM coastal agricultural plain have NO_3 concentrations exceeding the threshold of anthropogenic inputs, and most NO_3 concentrations in groundwater are above the drinking water limit of 50 mg/L. The isotopic composition of NO_3 revealed different anthropogenic sources contribute to NO_3 contamination of the local groundwater with manure, sewage, and soil organic as the potential NO_3 sources. Nonetheless, the $\delta^{11}B$ values indicate that NO_3 is chiefly derived from manure. The Bayesian isotope MixSIAR model results support manure as the major source of NO_3 to these groundwaters. The present study highlights the usefulness of $\delta^{11}B$ to separate nitrate and other contaminants from sewage and manure, because $\delta^{15}N_{NO3}$ and $\delta^{18}O_{NO3}$ values are commonly not capable of differentiating these sources and are often masked by various simultaneously occurring NO_3 transformation processes. Evidence of denitrification and nitrification are observed with heterogenous occurrence/distribution within the OGM groundwater system, reflecting the complexity of the study area, which is also influenced by seawater intrusion.

The measured NO_3 concentrations in the collected groundwater samples are two times higher than that measured previously in 2010. This suggests the existence of continuous sources of NO_3 that are deteriorating groundwater quality in the OGM aquifer.

Adaptation and mitigation strategies are required to improve the groundwater quality in the future. Optimization strategies, including an introduction of environmentally safe agricultural practices and an implementation of regulations for managing wastewater, are encouraged to achieve a sustainable management of this economically strategic agricultural area. The present study highlights the elevated NO_3 concentrations measured in the GEM Lagoon with potential contribution of NO_3 via interactions between groundwater of the OGM aquifer and surface water of the GEM Lagoon. This issue is of particular importance because input of nutrients to the GEM Lagoon can lead to eutrophication limiting its biodiversity.

Acknowledgements

The authors thank the Natural Sciences and Engineering Research Council of Canada for funding this project through NSERC Discovery Grants RGPIN-07117 and RGPIN-03766 held by Prof. Romain Chesnaux and Prof. Bernhard Mayer, respectively. The authors thank the local population of the OGM region who offered free access to their private wells during fieldwork. The authors would like to thank Mr. Mohamed Khwatmia from the National Center for Nuclear Sciences and Technologies (Tunisia) for his much-appreciated help during fieldwork. Ms. Stefanie Schmidt is thanked for her assistance in performing the chemical analyses at the Technical University of Darmstadt in Germany.

Credit author statement

The initial draft of the manuscript was written by Dr. Lamine Boumaiza and the co-authors commented on previous versions of the manuscript. All the authors approved the final version of the manuscript.

.Supplemental Table S1: Chemical and isotopic data

ID	pH	DO (mg/L)	T (°C)	EC (µS/cm)	TDS (mg/L)	Ca (mg/L)	Mg (mg/L)	Na (mg/L)	K (mg/L)	Cl (mg/L)	SO_4 (mg/L)	Br (mg/L)	NO_3 (mg/L)	HCO_3 (mg/L)	B (mg/L)	CBE (%)
1	7.4	0	20.9	1937	973	84.4	44.5	339.7	8.4	369.8	126.6	1.6	3.9	264.7	0.86	13
2	7.63	6.98	21.8	3620	1872	377.9	57.2	391.0	4.2	760.1	326.4	2.3	272.9	93.9	0.18	9
3	7.62	0	20.7	3140	1611	393.9	51.7	289.1	4.2	601.8	367.5	2.1	189.0	75.6	0.14	12
4	7.48	0	20.4	2950	1507	358.5	52.6	220.4	12.3	618.0	199.2	1.9	177.0	152.5	0.13	9
5	7.26	0	21.3	4380	2280	376.6	66.5	564.0	5.9	925.7	576.2	2.8	87.0	80.5	0.52	9
6	7.14	0	23	6590	3490	238.9	57.8	1213.0	14.2	1767.8	444.9	5.7	74.2	115.9	2.95	6
7	7.37	3.05	19.4	5760	3030	405.2	121.1	851.8	7.8	1438.6	531.4	3.8	25.3	96.4	0.04	11
8	7.55	3.33	22.3	2630	1338	169.6	71.5	215.7	5.5	503.9	154.8	1.9	377.7	108.6	0.17	3
9	7.5	5.95	18.5	5250	2760	496.0	121.3	583.4	6.7	1207.6	628.0	3.5	85.2	85.4	0.45	9
10	7.14	0.21	21.8	3940	2040	357.0	120.6	401.6	13.4	1028.4	230.9	3.3	149.3	107.4	0.25	12
11	7.47	0	20.6	5010	2630	478.3	99.0	612.0	3.5	1174.0	666.6	3.1	61.7	90.3	1.72	9
12	7.37	0.74	21.4	1841	922	142.0	33.0	273.7	2.0	251.5	195.0	1.2	152.0	184.2	0.16	13
13	7.05	0.95	21.8	2910	1496	253.3	37.0	325.3	11.8	566.6	362.7	2.0	114.1	95.2	0.60	6
14	7.24	6.81	19.6	2580	1311	239.2	60.1	240.1	7.2	495.5	157.1	1.8	127.7	87.8	0.16	14
15	7.32	0	23	1280	634	127.2	18.8	137.5	2.7	286.7	38.1	1.1	43.4	87.8	0.54	12
16	7.31	5.64	21.6	1272	629	102.4	33.6	145.7	5.3	231.7	90.8	0.9	19.8	128.1	0.14	14
17	7.22	0	20.3	2760	1406	269.2	83.4	271.2	8.9	466.0	187.5	1.4	489.1	92.7	0.26	10
18	7.28	0	20.5	1853	928	82.3	45.5	200.3	7.7	311.8	165.7	1.2	69.3	118.3	0.25	4
19	7.39	0	21.3	2350	1187	281.0	67.0	245.0	5.8	516.2	191.7	1.6	216.6	93.9	0.25	12
20	7.17	0	22.2	7980	4280	186.8	168.4	1400.1	46.8	2337.8	297.0	8.7	31.6	87.8	0.34	7
21	7.59	4.5	21.1	4290	2250	133.9	90.3	704.1	24.1	1209.7	171.3	4.9	3.8	162.3	0.40	6
GEM	7.19	6.46	25.1	60300	39200	271.2	1570.1	13491.2	560.4	20109.5	3399.1	88.1	86.8	173.2	3.87	7
MS	7.4	8.45	23.8	50200	33300	189.4	1342.7	11670.6	520.8	17863.4	3198.9	80.3	104.1	179.3	5.08	5

Note: CBE is the Charge Balance Error, which is verified for the whole of analyzed samples with mean CBE $\leqslant$10%. Here, the mean CBE is about 9%.

Supplemental Table S1: Chemical and isotopic data (continue)

ID	$\delta^{18}O_{H2O}$ (‰VSMOW)	$\delta^{2}H_{H2O}$ (‰VSMOW)	d-excess (‰)	$\delta^{15}N_{NO3}$ (‰AIR)	$\delta^{18}O_{NO3}$ (‰VSMOW)	Theoretical $\delta^{18}O_{NO3}$ (‰)	$\Delta\delta^{18}O_{NO3}$ (‰)	Contribution of NO_3 (%)[1]	$\delta^{11}B$ (‰ NBS-951)
1	-5.7	-30.9	14.6	13.7	12.9	4.0	8.9	31	29.7
2	-4.8	-28.1	10.3	7.3	6.1	4.6	1.4	76	35.9
3	-4.8	-26.9	11.8	-	-	4.6	-	-	37.5
4	-4.5	-25.9	10.2	5.8	6.0	4.8	1.2	81	34.3
5	-4.2	-24.5	9.1	5.9	6.7	5.0	1.7	75	27.4
6	-5.7	-32.1	13.3	4.7	5.7	4.0	1.6	71	13.6
7	-4.4	-25.5	10.0	11.7	15.6	4.9	10.8	31	34.8
8	-5.3	-31.2	11.2	7.4	10.1	4.3	5.8	42	39.8
9	-4.2	-24.3	9.1	8.8	8.9	5.0	3.9	57	33.8
10	-4.5	-26.5	9.8	5.2	6.5	4.8	1.7	74	29.3
11	-4.1	-24.8	8.0	7.3	8.9	5.1	3.8	58	12.4
12	-5.0	-27.1	12.8	8.9	4.1	4.5	-0.4	-	35.4
13	-4.8	-26.9	11.9	6.3	9.1	4.6	4.5	51	42.9
14	-4.9	-26.2	12.6	6.0	6.5	4.6	1.9	71	36.4
15	-5.5	-29.7	14.2	6.7	4.7	4.2	0.6	88	24.1
16	-5.5	-29.7	14.3	6.8	8.4	4.2	4.2	50	33.5
17	-5.5	-30.4	13.6	8.6	6.4	4.2	2.3	65	30.0
18	-5.1	-27.6	13.0	8.1	7.9	4.5	3.5	56	42.6
19	-5.4	-30.8	12.2	6.1	7.7	4.3	3.4	55	41.2
20	-5.1	-27.2	13.8	11.7	14.8	4.4	10.3	30	27.4
21	-5.4	-28.7	14.8	6.8	7.3	4.2	3.1	57	37.7
GEM	1.4	9.7	-0.6	-	-	-	-	-	42.3
MS	1.3	9.5	-1.1	-	-	-	-	-	41.4

1: Contribution of nitrate from nitrification is the portion of the theoretical $\delta^{18}O_{NO3}$ (‰) relative to the measured $\delta^{18}O_{NO3}$ (‰).

Supplementary Figures S1a-d: Correlation of different chemical and isotopic values. In Figure S2, a positive trend is indicated based on groundwater samples traced with blue circles, whereas red triangle are groundwater samples that are not considered.

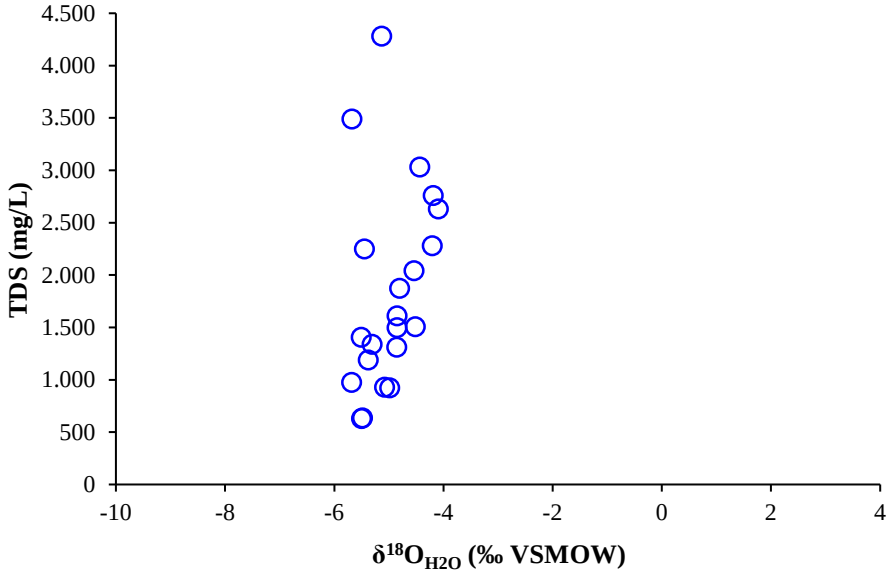

Supplemental Figure S1a

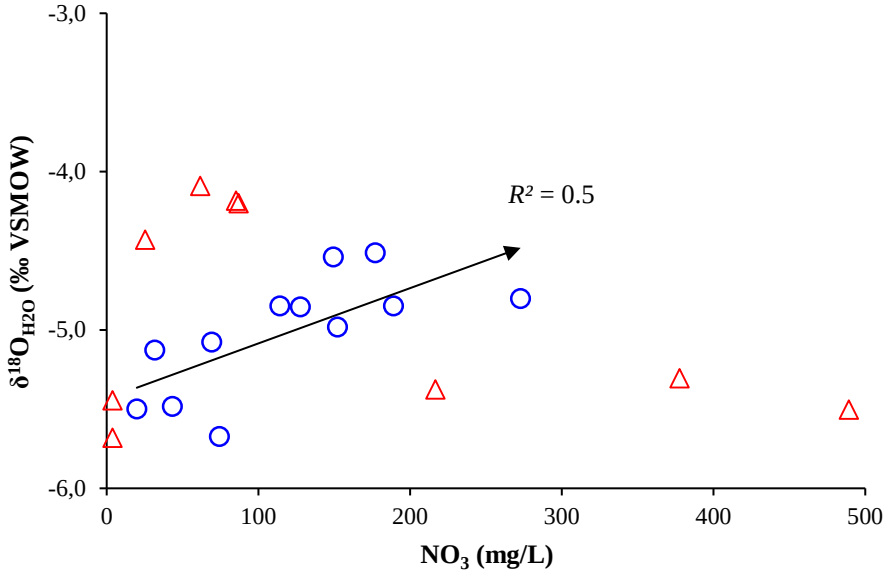

Supplemental Figure S1b

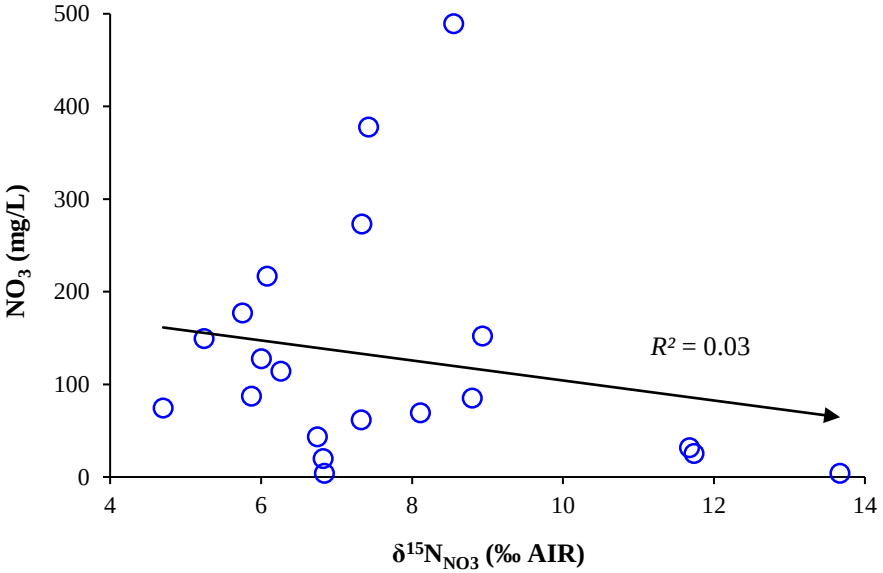

Supplemental Figure S1c

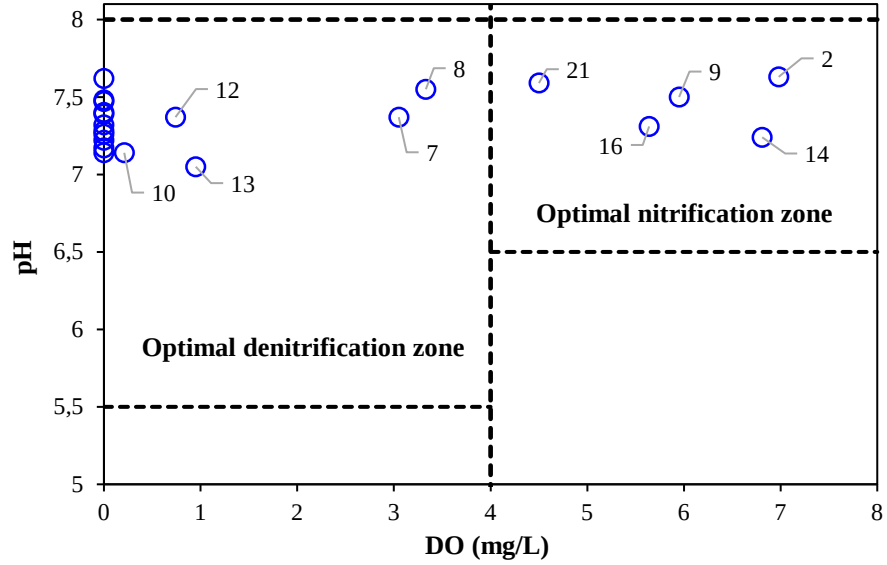

Supplemental Figure S1d

Supplementary Figure S2. General piezometric map of the study area (adapted from Ben Ammar et al. (2016).

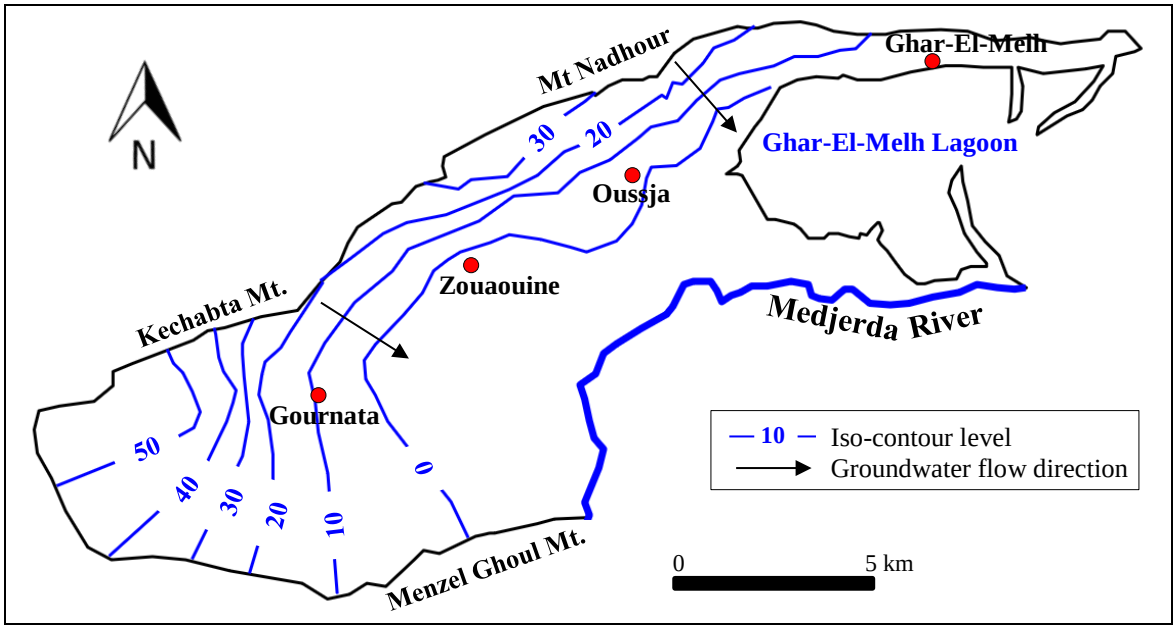

References

Aissaoui, A., 2020. Sowing seeds in Tunisian sands. Food and Agriculture Organization of United Nations (www.fao.org/fao-stories/article/en/c/1287893/).

Aravena, R., Mayer, B., 2010. Isotopes and processes in the nitrogen and sulfur cycles, in: Environmental Isotopes in Biodegradation and Bioremediation. pp. 203–246.

Ayache, F., Thompson, J.R., Flower, R.J., Boujarra, A., Rouatbi, F., Makina, H., 2009. Environmental characteristics, landscape history and pressures on three coastal lagoons in the Southern Mediterranean Region: Merja Zerga (Morocco), Ghar El Melh (Tunisia) and Lake Manzala (Egypt). Hydrobiologia 622, 15–43.

Ben Ammar, S., Taupin, J.D., Ben Alaya, M., Zouari, K., Patris, N., Khouatmia, M., 2020. Using geochemical and isotopic tracers to characterize groundwater dynamics and salinity sources in the Wadi Guenniche coastal plain in northern Tunisia. J. Arid Environ. 178, 1–14.

Ben Ammar, S., Taupin, J.D., Zouari, K., Khouatmia, M., 2016. Identifying recharge and salinization sources of groundwater in the Oussja Ghar el Melah plain (northeast Tunisia) using geochemical tools and environmental isotopes. Environ. Earth Sci. 75, 1–16.

Blarasin, M., Cabrera, A., Ioannis Matiatos, I., Becher Quinodóz, F., Giuliano Albo, J., Lutri, V., Matteoda, E., Panarello, H., 2020. Comparative evaluation of urban versus agricultural nitrate sources and sinks in an unconfined aquifer by isotopic and multivariate analyses. Sci. Total Environ. 741, 1–15.

Blarasin, M., Cabrera, A., Matteoda, E., 2014. Aguas subterráneas de la provincia de Córdoba, Argentina. UniRío. Río Cuarto.

Böttcher, J., Strebel, O., Voerkelius, S., Schmidt, H.L., 1990. Using isotope fractionation of nitrate-nitrogen and nitrate-oxygen for evaluation of microbial denitrification in a sandy aquifer. J. Hydrol. 114, 413–424.

Bouchouicha, S., 2004. Étude Hydrogéologique de la Nappe Utique-Aousja. Vulnérabilité et établissement des Périmètres de Protection. Mémoire de Maitrise, Université de Bizerte, Bizerte, Tunisie.

Boumaiza, L., Chabour, N., Drias, T., 2019. Reviewing the potential anthropogenic sources of groundwater contamination - Case study of the expanding urban area of Taleza in Algeria, in: Proceedings of the 72nd Canadian Geotechnical Conference (GeoSt-John's 2019), Saint-John's, Newfoundland and Labrador, Canada,. p. 9.

Boumaiza, L., Chesnaux, R., Drias, T., Walter, J., Huneau, F., Garel, E., Knoeller, K., Stumpp, C., 2020. Identifying groundwater degradation sources in a Mediterranean coastal area experiencing significant multi-origin stresses. Sci. Total Environ. 746, 1–20.

Boumaiza, L., Chesnaux, R., Walter, J., Drias, T., Huneau, F., Garel, E., Vystavna, Y., Stumpp, C., 2021. Reviewing the anthropogenic sources of groundwater contamination in the Plain of the El-Nil River, Algeria, in: Proceedings of the 74th Canadian Geotechnical Conference and the 14th Joint CGS/IAH-CNC Groundwater Conference (GeoNiagara-2021), Niagara Falls, Ontario, Canada. p. 9.

Boumaiza, L., Walter, J., Chesnaux, R., Huneau, F., Garel, E., Erostate, M., Johannesson, K.H., Vystavna, Y., Bougherira, N., Bordeleau, G., Stotler, R.L., Blarasin, M., Gutierrez, M., Knöller, K., Stumpp, C., 2022a. Multi-tracer approach to understand

nitrate contamination and groundwater-surface water interactions in the Mediterranean coastal area of Guerbes-Senhadja, Algeria. J. Contam. Hydrol. 251, 1–16.

Boumaiza, L., Walter, J., Chesnaux, R., Zahi, F., Huneau, F., Garel, E., Stotler, R.L., Bordeleau, G., Drias, T., Johannesson, K.H., Vystavna, Y., Re, V., Knöller, K., Stumpp, C., 2022b. Combined effects of seawater intrusion and nitrate contamination on groundwater in coastal agricultural areas: A case from the Plain of the El-Nil River (North-Eastern Algeria). Sci. Total Environ. 851, 1–13.

Bouzourra, H., Bouhlila, R., Elango, L., Slama, F., Ouslati, N., 2015. Characterization of mechanisms and processes of groundwater salinization in irrigated coastal area using statistics, GIS, and hydrogeochemical investigations. Environ. Sci. Pollut. Res. 22, 2643–2660.

Brookfield, A.E., Hansen, A.T., Sullivan, P.L., Czuba, J.A., Kirk, M.F., Li, L., Newcomer, M.E., Wilkinson, G., 2021. Predicting algal blooms: Are we overlooking groundwater? Sci. Total Environ. 769, 1–15.

Burrolet, P.F., Dumon, E., 1952. Geological map of Porto Farina. National Office of Mines, Tunisia.

Carrubba, S., 2017. Cartographie des vulnérabilités de l'aquifère côtier de Ghar El Melh en Tunisie. Strategic Partnership for the Mediterranean Sea Large Marine Ecosystem (MedPartnership), Project Report.

Carrubba, S., 2014. Vulnerability mapping of the Ghar El Melh coastal aquifer in Tunisia. Strategic Partnership for the Mediterranean Sea Large Marine Ecosystem (MedPartnership), Project Report.

Casciotti, K.L., Sigman, D.M., Hastings, M.G., Böhlke, J.K., Hilkert, A., 2002. Measurement of the oxygen isotopic composition of nitrate in seawater and freshwater using the denitrifier method. Anal. Chem. 74, 4905–4912.

Celle, H., 2000. Caractérisation des précipitations sur le pourtour de la Méditerranée occidentale. Approche isotopique et chimique. PhD thesis, Université d'Avignon, France.

Chafouq, D., El Mandour, A., Elgettafi, M., Himi, M., Chouikri, I., Casas, A., 2018. Hydrochemical and isotopic characterization of groundwater in the Ghis-Nekor plain (northern Morocco). J. African Earth Sci. 139, 1–13.

Chelbi, F., Paskoff, R., Trousset, P., 1995. La baie d'Utique et son évolution depuis l'Antiquité: une réévaluation géoarchéologique. Antiq. africaines 31, 7–51.

Chen, D.J.Z., MacQuarrie, K.T.B., 2005. Correlation of δ15N and δ18O in NO3−during denitrification in groundwater. J. Environ. Eng. Sci. 4, 221–226.

Clark, I.D., Fritz, P., 1997. Environmental isotopes in hydrogeology. CRC Press-Lewis Publishers.

Craig, H., 1961. Isotopic variations in meteoric waters. Science (80-.). 133, 1702–1703.

Elmeknassi, M., Bouchaou, L., El Mandour, A., Elgettafi, M., Himi, M., Casas, A., 2022. Multiple stable isotopes and geochemical approaches to elucidate groundwater salinity and contamination in the critical coastal zone: A case from the Bou-areg and Gareb aquifers (North-Eastern Morocco). Environ. Pollut. 300, 1–13.

Erostate, M., Huneau, F., Garel, E., Lehmann, M.F., Kuhn, T., Aquilina, L., Vergnaud-Ayraud, V., Labasque, T., Santoni, S., Robert, S., Provitolo, D., Pasqualini, V., 2018. Delayed nitrate dispersion within a coastal aquifer provides constraints on

land-use evolution and nitrate contamination in the past. Sci. Total Environ. 644, 928–940.
Fukada, T., Hiscock, K.M., Dennis, P.F., 2004. A dual-isotope approach to the nitrogen hydrochemistry of an urban aquifer. Appl. Geochemistry. https://doi.org/10.1016/j.apgeochem.2003.11.001
Gaillardet, J., Lemarchand, D., Göpel, C., G., M., 2001. Evaporation and sublimation of boric acid: application for boron purification from organic rich solutions. Geostand. Newsl. 25, 67–75.
Gomez Isaza, D.F., Cramp, R.L., Franklin, C.E., 2020. Living in polluted waters: A meta-analysis of the effects of nitrate and interactions with other environmental stressors on freshwater taxa. Environ. Pollut. 261, 1–12.
Guerrot, C., Millot, R., Robert, M., Negrel, P., 2011. Accurate and High-Precision Determination of Boron Isotopic Ratios at Low Concentration by MC-ICP-MS (Neptune). Geostand. Geoanalytical Res. 35, 275–284.
Gutiérrez, M., Biagioni, R.N., Alarcòn-Herrera, M.T., Rivas-Lucero, B.A., 2018. An overview of nitrate sources and operating processes in arid and semiarid aquifer systems. Sci. Total Environ. 624, 1513–1522.
Harvey, F.E., Sibray, S.S., 2001. Delineating Ground Water Recharge from Leaking Irrigation Canals Using Water Chemistry and Isotopes. Groundwater 39, 408–421.
He, S., Li, P., Su, F., Wang, D., Ren, X., 2022. Identification and apportionment of shallow groundwater nitrate pollution in Weining Plain, northwest China, using hydrochemical indices, nitrate stable isotopes, and the new Bayesian stable isotope mixing model (MixSIAR). Environ. Pollut. 298, 1–11.
Hendry, M.J., McCready, R.G.L., Gould, W.D., 1984. Distribution, source and evolution of nitrate in a glacial till of southern Alberta, Canada. J. Hydrol. 70, 177–198.
Holloway, J.M., Dahlgren, R.A., 2002. Nitrogen in rock: Occurrences and biogeochemical implications. Global Biogeochem. Cycles 14, 1–17.
Jacks, G., Sharma, V.P., 1983. Nitrogen circulation and nitrate in groundwater in an agricultural catchment in southern India. Environ. Geol. 5, 61–64.
Jia, Y., Guo, H., Xi, B., Jiang, Y., Zhang, Z., Yuan, R., Yi, W., Xue, X., 2017. Sources of groundwater salinity and potential impact on arsenic mobility in the western Hetao Basin. Sci. Total Environ. 601, 691–702.
Jin, Z., Qin, X., Chen, L., Jin, M., Li, F., 2015. Using dual isotopes to evaluate sources and transformations of nitrate in the West Lake watershed, eastern China. J. Contam. Hydrol. 177, 64–75.
Kaown, D., Koh, D.C., Mayer, B., Mahlknecht, J., Ju, Y., Rhee, S.K., Kim, J.H., Park, D.K., Park, I., Lee, H.L., Yoon, Y.Y., Lee, K.K., 2023. Estimation of nutrient sources and fate in groundwater near a large weir-regulated river using multiple isotopes and microbial signatures. J. Hazard. Mater. 446, 1–13.
Kendall, C., 1998. Tracing Nitrogen Sources and Cycling in Catchments. Isot. Tracers Catchment Hydrol. 519–576.
Kendall, C., Elliott, E.M., Wankel, S.D., 2007. Tracing Anthropogenic Inputs of Nitrogen to Ecosystems, Chapter 12, In: R.H. Michener and K. Lajtha (Eds.). Stable Isot. Ecol. Environ. Sci. Second Ed. Blackwell Publ. 375–449.
Komor, S.C., 1997. Boron contents and isotopic composition of hog manure, selected fertilizers, and water in Minnesota. J. Environ. Qual. 26, 1212–1222.

Kruk, M.K., Mayer, B., Nightingale, M., Laceby, J.P., 2020. Tracing nitrate sources with a combined isotope approach (δ15NNO3, δ18ONO3 and δ11B) in a large mixed-use watershed in southern Alberta. Sci. Total Environ. 703, 1–15.

Lane, A.D., Kirk, M.F., Whittemore, D.O., Stotler, R., Hildebrand, J., Feril, O., 2020. Long-term (1970s–2016) changes in groundwater geochemistry in the High Plains aquifer in south-central Kansas, USA. Hydrogeol. J. 28, 491–501.

Lasagna, M., De Luca, D.A., 2017. Evaluation of sources and fate of nitrates in the western Po plain groundwater (Italy) using nitrogen and boron isotopes. Environ. Sci. Pollut. Res. 26, 2089–2104.

Mahlknecht, J., Horst, A., Hernández-Limón, G., Aravena, R., 2008. Groundwater geochemistry of the Chihuahua City region in the Rio Conchos Basin (northern Mexico) and implications for water resources management. Hydrol. Process. 22, 4736–4751.

Malki, M., Bouchaou, L., Hirich, A., Ait Brahim, Y., Choukr-Allah, R., 2017. Impact of agricultural practices on groundwater quality in intensive irrigated area of Chtouka-Massa, Morocco. Sci. Total Environ. 574, 760–770.

MAT, (Ministère de l'Agriculture de la Tunisie), 2006. Rapports techniques des piézomètres et des forages - Annuaires de surveillance piézométrique 1971-2006. inistère de l'Agriculture de la Tunisie, Tunisie.

Matiatos, I., 2016. Nitrate source identification in groundwater of multiple land-use areas by combining isotopes and multivariate statistical analysis: A case study of Asopos basin (Central Greece). Sci. Total Environ. 541, 802–814.

MDDELCC, (Ministère du Développement durable de l'Environnement et de la Lutte contre les changements climatiques), 2015. Guide technique sur le traitement des eaux usées des résidences isolées. Règlement sur l'évacuation des eaux usées des résidences isolées. Québec, Canada.

Melki, F., Zouaghi, T., Harrab, S., Casas Sainz, A., Bedir, M., Zargouni, F., 2011. Structuring and evolution of Neogene transcurrent basins in the Tellian foreland domain, north-eastern Tunisia. J. Geodyn. 52, 57–69.

Mills, T.J., Mast, M.A., Thomas, J., Keith, G., 2016. Controls on selenium distribution and mobilization in an irrigated shallow groundwater system underlain by Mancos Shale, Uncompahgre River Basin, Colorado, USA. Sci. Total Environ. 566–567, 1621–1631.

Moon, H.S., Komlos, J., Jaffé, P.R., 2007. Uranium reoxidation in previously bioreduced sediment by dissolved oxygen and nitrate. Environ. Sci. Technol. 41, 4587–4592.

Moore, K.B., Ekwurzel, B., Esser, B.K., Hudson, G.B., Moran, J.., 2006. Sources of groundwater nitrate revealed using residence time and isotope methods. Appl. Geochemistry 21, 1016–1029.

Moussaoui, I., Rosa, E., Cloutier, V., Neculita, C.M., Dassi, L., 2023. Chemical and isotopic evaluation of groundwater salinization processes in the Djebeniana coastal aquifer, Tunisia. Appl. Geochemistry 149, 1–13.

Nikolenko, O., Jurado, A., Borges, A.V., Knöller, K., Brouyère, S., 2018. Isotopic composition of nitrogen species in groundwater under agricultural areas: a review. Sci. Total Environ. 621, 1415–1432.

Ogrinc, N., Tamse, S., Zavadlav, S., Vrzel, J., Jin, L., 2019. Evaluation of geochemical processes and nitrate pollution sources at the Ljubljansko polje aquifer (Slovenia):

a stable isotope perspective. Sci. Total Environ. 646, 1588–1600.
Ouerghi, S., 2021. A GIS-based Assessment of the Vulnerability to Potential Pollution of the Alluvial Aquifer of Aousja-Ghar El Melh (North-East of Tunisia) Using the Parametric Method DRASTIC. Eur. J. Eng. Technol. Res. 6, 81–87.
Parnell, A.C., Inger, R., Bearhop, S., Jackson, A.L., 2010. Source partitioning using stable isotopes: coping with too much variation. PLoS One 5(3):e9672. https://doi.org/10.1371/journal.pone.0009672
Penna, D., Stenni, B., Šanda, M., Wrede, S., Bogaard, T.A., Gobbi, A., Borga, M., Fischer, B.M.C., Bonazza, M., Chárová, Z., 2010. On the reproducibility and repeatability of laser absorption spectroscopy measurements for δ 2 H and δ 18 O isotopic analysis. Hydrol. Earth Syst. Sci. 14, 1551–1566.
Pimienta, J., 1959. Le cycle pliocène-actuel dans les bassins paraliques de Tunis. Mémoires de la Société Géologique de France, No. 85, Paris, France.
Puig, R., Soler, A., Widory, D., Mas-Pla, J., Domènech, C., Otero, N., 2017. Characterizing sources and natural attenuation of nitrate contamination in the BaixTer aquifer system (NE Spain) using a multi-isotope approach. Sci. Total Environ. 580, 518–532.
Pulido-Bosch, A., Rigol-Sanchez, J.P., Vallejos, A., Andreu, J.M., Ceron, J.C., Molina-Sanchez, L., Sola, F., 2018. Impacts of agricultural irrigation on groundwater salinity. Environ. Earth Sci. 77, 1–14.
Re, V., Kammoun, S., Sacchi, E., Trabelsi, R., Zouari, K., Matiatos, I., Allais, E., Daniele, S., 2021. A critical assessment of widely used techniques for nitrate source apportionment in arid and semi-arid regions. Sci. Total Environ. 775, 1–12.
Re, V., Sacchi, E., 2017. Tackling the salinity-pollution nexus in coastal aquifers from arid regions using nitrate and boron isotopes. Environ. Sci. Pollut. Res. 24, 13247–13261.
Saadaoui, M., 1983. Note sur L'hydrologie du Lac de Ghar el Melh. Bureau de l'inventaire et de Recherches Hydrologiques, Tunisie.
Santoni, S., Huneau, F., GAREL, E., Celle-Jeanton, H., 2018. Multiple recharge processes to heterogeneous Mediterranean coastal aquifers and implications on recharge rates evolution in time. J. Hydrol. 559, 669–683.
Scanlon, B.R., Reedy, R.C., Bronson, K.F., 2008. Impacts of Land Use Change on Nitrogen Cycling Archived in Semiarid Unsaturated Zone Nitrate Profiles, Southern High Plains, Texas. Environ. Sci. Technol. 42, 1–7.
Schroeder, A., Souza, D.H., Fernandes, M., Rodrigues, E.B., Trevisan, V., Skoronski, E., 2020. Application of glycerol as carbon source for continuous drinking water denitrification using microorganism from natural biomass. J. Environ. Manage. 256, 109964–109971.
Sigman, D.M., Casciotti, K.L., Andreani, M., Barford, C., Galanter, M., Böhlke, J.K., 2001. A bacterial method for the nitrogen isotopic analysis of nitrate in seawater and freshwater. Anal. Chem. 73, 4145–4153.
Singleton, M.J., Esser, B.K., Moran, J.E., Hudson, G.B., Mcnab, W.W., Harter, T., 2007. Saturated zone denitrification: Potential for natural attenuation of nitrate contamination in shallow groundwater under dairy operations. Environ. Sci. Technol. 41, 759–765.
Stock, B.C., Jackson, A.L., Ward, E.J., Parnell, A.C., Phillips, D.L., Semmens, B.X., 2018.

Analyzing mixing systems using a new generation of Bayesian tracer mixing models. PeerJ 6, e5096. https://doi.org/https://doi.org/10.7717/peerj.5096.

Sutton, M.A., Howard, C.M., Erisman, J.W., Billen, G., Bleeker, A., Grennfelt, P., Van Grinsven, H., Grizzetti, B., 2011. The European Nitrogen Assessment, The European Nitrogen Assessment. Cambridge University Press.

Torres-Martínez, J.A., Mora, A., Mahlknecht, J., Daessle, L.W., Cervantes-Aviles, P.A., Ledesma-Ruiz, R., 2021. Estimation of nitrate pollution sources and transformations in groundwater of an intensive livestock-agricultural area (Comarca Lagunera), combining major ions, stable isotopes and MixSIAR model. Environ. Pollut. 269, 1–12.

Vengosh, A., Heumann, K.G., Juraske, S., Kasher, R., 1994. Boron isotope application for tracing sources of contamination in groundwater. Environ. Sci. Technol. 28, 1968–1974.

Vystavna, Y., Diadin, D., Yakovlev, V., Hejzlar, J., Vadillo, I., Huneau, F., Lehmann, M.F., 2017. Nitrate contamination in a shallow urban aquifer in East Ukraine: evidence from hydrochemical, stable isotopes of nitrate and land use analysis. Environ. Earth Sci. 76, 1–13.

Ward, M., Jones, R., Brender, J., De Kok, T., Weyer, P., Nolan, B., Van Breda, S., 2018. Drinking water nitrate and human health: an updated review. Int. J. Environ. Res. Public Health 15, 1–31.

Weeks, E.P., McMahon, P.B., 2007. Nitrous Oxide Fluxes from Cultivated Areas and Rangeland: U.S. High Plains. Vadose Zo. J. 6, 496–510.

WHO, (World Health Organization), 2017. Guidelines for drinking-water quality, 4th edition, incorporating the 1st addendum. ISBN: 978-92-4-154995-0.

Yeshno, E., Arnon, S., Dahan, O., 2019. Real-time monitoring of nitrate in soils as a key for optimization of agricultural productivity and prevention of groundwater pollution. Hydrol. Earth Syst. Sci. 23, 3997–4010.

Zendehbad, M., Cepuder, P., Loiskandl, W., Stumpp, C., 2019. Source identification of nitrate contamination in the urban aquifer of Mashhad, Iran. J. Hydrol. Reg. Stud. 25, 1–14.

Zhang, Y., Li, F., Zhang, Q., Li, J., Liu, Q., 2014. . Tracing nitrate pollution sources and transformations in surface- and ground-waters using environmental isotopes. Sci. Total Environ. 490, 213–222.